2018 European Control Conference (ECC)
June 12-15, 2018. Limassol, Cyprus

Distributed model predictive control for building demand-side management

Alessandra Parisio, Salvador Pacheco Gutierrez

Abstract— **Demand-side management is widely acknowledged as an important source of flexibility and then an essential element to balance supply and demand more effectively. A fundamental challenge is to enable buildings to participate in demand-side services without violating indoor comfort. In this paper, we present a hierarchical Model Predictive Control (MPC) approach to demand-side management in buildings, which encompasses heating/cooling systems, onsite generation and storage technologies, and enables the building to participate in balancing programs. In the upper level, a trajectory planner calculates the best possible reachable power profile to track as reference. In the lower level, a tracking problem is solved, which also minimises the energy use without violating the indoor comfort. The tracking problem is formulated so that an active-set method can be applied and the MPC problem can be solved in a distributed manner. Numerical results with real data from one university building show the promising performance and computational tractability of the proposed approach, which can enable practical implementations on building platforms.**

I. Introduction

In order to smarten the energy grid, significant research is to be devoted to buildings due to their large share of energy use, and the fact that they can increasingly integrate not just inelastic loads, but also distributed generation, storage resources and flexible loads [1]. Despite the recent advances in the area of energy management systems for intelligent buildings, significant effort is still required [2]. Predictive automation systems are becoming available as expensive tailored configurations with limited functionalities (e.g., Ecopilot, GridEdge, Verdigrid), which do not achieve the expected theoretical results, whilst holistic and standardised solutions are not available yet [2]. This paper addresses the need of providing an overarching control framework that optimally coordinates heating/cooling systems, onsite generation, and storage, with the grid signal. The proposed control framework adopts a distributed approach, which is beneficial for implementation on real platforms.

Literature review: Among the various approaches adopted within the energy management literature, such as game theory and approximate dynamic programming, Model Predictive Control (MPC) [3] has received particular attention, because of its capability to integrate economic, social and environmental aspects, handle the future behavior of the system, compute control actions based on an optimal control problem including technical and operating constraints, as well as make the controlled system more robust against uncertainty [4], [2]. Decentralised and distributed Model Predictive Control (MPC) frameworks have been proposed for controlling Heating, Ventilation and Air Conditioning (HVAC) systems (e.g., [5], [6]), which commonly either consider decoupled thermal zones ([5]) or apply the method of alternating direction method of multipliers (ADMM) ([6]). Some studies have demonstrated the potential benefits of MPC frameworks also for buildings-to-grid applications, in particular for frequency service provision of HVAC systems (e.g., [7]). There are a few studies showing promising results in reducing costs and peak power of centralised MPC schemes for residential buildings including heat pumps [8], which however simply model the thermal building dynamics considering one aggregated thermal zone. There are not studies in the literature targeting the design of advanced building control schemes extended both in terms of assets under control, i.e., distributed generators and storage systems, and functions (ancillary services) [4].

Statement of Contributions: Designing efficient controllers for complex systems such as buildings is demanding. MPC strategies offer a promising solution but generally come with computational issues, since they require solving large-scale optimisation problems in real time. An efficient solution is to distribute the computational requirements over multiple units, but this can lead to high communication costs. Building on the work of [9], [10], we propose a distributed MPC control framework that integrates and optimally coordinates demand response, onsite generation and energy storage. By doing so the building will be able to offer ancillary services to the grid operator without violating indoor comfort. Theoretical and experimental results demonstrate that the distributed implementation of the active-set method in [9] outperforms dual decomposition and ADMM especially in building control applications, requiring much smaller number of iterations to converge and significantly reducing the computation time [10]. In this paper, we address the problem of coordinating and optimising demand-side services, onsite generation and energy storage technologies along with along with more standard objectives (e.g., control of the indoor air quality). We show that this problem can be formulated such that the active-set method in [9] can be applied and implemented in a distributed fashion. Furthermore, we propose a suitable initialisation algorithm.

Outline of the manuscript: Section II presents the model of the building and its onsite generation, while Section III describes the distributed MPC algorithm. Section **??** provides and discusses numerical results, while Section V summarizes

A. Parisio, S. Pacheco Gutierrez are with the School of Electrical & Electronic Engineering, University of Manchester, M13 9PL, United Kingdom. The research leading to these results was supported by the Innovate UK Internet of Things cities Demonstrator: CityVerve. Corresponding author: alessandra.parisio@manchester.ac.uk.

our conclusions and proposes future directions.

A. Nomenclature

Tables I reports parameters and variables defined in the proposed control framework. In this study we consider discrete-time dynamical systems with a Δk sampling time. Power variables represent the average power over the given sampling period. For simplicity we omit the subscript denoting the time k in Table I.

TABLE I: Decision variables and parameters involved in the algorithm

$P^{\text{gas,B}}/P^{\text{gas,CHP}}$	micro-CHP/boiler gas power input
P^{HP}	heat pump electrical power input
$\dot{Q}^{\text{i,heat}}$	heat power input to thermal zone i
$T^{\text{i,a}}/T^{\text{s}}$	average temperature of the indoor air of thermal zone i/of the thermal storage
$\Delta P^{\text{UP}}/\Delta P^{\text{DOWN}}$	power increase/decrease with respect to the baseline
$\Delta P^{\text{gas,CHP}}$	change in the micro-CHP gas power input with respect to the baseline
$\Delta P^{\text{gas,B}}$	change in the boiler gas power input with respect to the baseline
ΔP^{HP}	change in the heat pump electrical power input with respect to the baseline
$\dot{Q}^{i,\text{heat}}$	change in the heat power input to thermal zone i with respect to the baseline
T	prediction horizon
N	number of thermal zones
$c^{\text{UP}}/c^{\text{DOWN}}$	economic incentives to increase/decrease the grid import at a given point in time
$\eta^{\text{e}}/\eta^{\text{h}}$	micro-CHP power/heat efficiency
η^{B}	boiler efficiency
COP	coefficient of performance of the heat pump
C^a/C^s	air/TES heat capacity
G	solar heat gain coefficient
$A^{\text{i,win}}/A^{\text{s}}$	windows area/TES exposed surface
I^{i}	incident solar radiation on the windows of thermal zone i
C	heat emission (per occupant)
$N^{\text{i,people}}$	number of occupants of thermal zone i
R^{i}	thermal resistance of thermal zone i
h^{s}	TES heat transfer coefficient
T^{ext}	outdoor temperature
$\underline{P}^{\text{HP}}, \overline{P}^{\text{HP}}$	bounds on heat pump electrical power
$\underline{P}^{\text{gas,CHP}}, \overline{P}^{\text{gas,CHP}}$	bounds on micro-CHP gas power
$\underline{T}^{\text{s}}, \overline{T}^{\text{s}}$	bounds on TES temperature
$\underline{T}^{\text{i,a}}, \overline{T}^{\text{i,a}}$	comfort bounds for thermal zone i

II. Modeling

In this section we outline the modeling of the main components considered in the proposed control framework.

Because of the scope of the paper and due to space constraints, we focus on the modeling of heating systems, thermal zones, micro-CHP and thermal energy storage (TES). The interested reader is referred to [11], [12], [13] and references therein for additional modeling details. We aim at using a control-orienting modeling framework, which can capture the main energy-related dynamics while keeping the number of states limited.

Thermal zones: We consider multiple thermal zones, each having a dedicated local computing unit. The temperature dynamics of each thermal zone i can be modeled by using a resistance-capacitance circuit analogy

$$C^a T^{\text{i,a}}_{k+1} = \frac{T^{\text{ext}}_k - T^{\text{i,a}}_k}{R^{\text{i}}} + CN^{\text{i,people}}_k + GA^{\text{i,win}} I^{\text{i}}_k + \dot{Q}^{\text{i,heat}}_k.$$

Remark 1: $\dot{Q}^{\text{i,heat}}$ can be expanded to specify the contributions coming from different units, such as the ventilation unit and floor heating (e.g., $\dot{Q}^{\text{i,heat}} = \dot{Q}^{\text{i,floor}} + \dot{Q}^{\text{i,vent}}$).

Heat pump: The behaviour of a heat pump at each time k is modeled as $\dot{Q}^{\text{HP}}_k = \text{COP} P^{\text{HP}}_k$, where $\dot{Q}^{\text{HP}}_k$ is the heat generated by the heat pump at time k and $\text{COP} = \eta \text{COP}^{\text{Carnot}}$. COP represents the technically feasible whilst the theoretically achievable COP is defined as $\text{COP}^{\text{Carnot}}$, with η denoting a quality grade.

Remark 2: For the sake of simplicity, in this study we discuss only the heating (winter) scenario. The proposed control framework can also easily include cooling by allowing for a negative $\dot{Q}^{\text{HP}}$ and forecasts of the energy efficiency ratio $\text{EER} = 1 - \text{COP}$.

Micro-CHP: The component represents a typical micro combined heat and power (micro-CHP) unit. The micro-CHP at each time k is described by the following equations: $P^{\text{CHP}}_k = \eta^{\text{e}} P^{\text{gas,CHP}}_k$ and $\dot{Q}^{\text{CHP}}_k = \eta^{\text{h}} P^{\text{gas,CHP}}_k$, where P^{CHP}_k and $\dot{Q}^{\text{CHP}}_k$ are respectively the electrical and heat power produced by the micro-CHP.

Boiler: A gas-based boiler is considered and modeled through its efficiency: $\dot{Q}^{\text{B}}_k = \eta^{\text{B}} P^{\text{gas,B}}_k$, where $\dot{Q}^{\text{B}}_k$ is the heat produced by the boiler. Electric boilers can be likewise included in the proposed framework.

Thermal energy storage: The dynamics of the TES can be expressed as

$$C^s T^{\text{s}}_{k+1} = \dot{Q}^{\text{s}}_k - \dot{Q}^{\text{load}}_k - \text{h}^{\text{s}}\text{A}^{\text{s}}(T^{\text{s}}_k - T^{\text{ext}}_k),$$

where $\dot{Q}^{\text{s}}_k = \dot{Q}^{\text{CHP}}_k + \dot{Q}^{\text{B}}_k + \dot{Q}^{\text{HP}}_k$ is the heat input to the storage, $\dot{Q}^{\text{load}}_k = \sum_{i=1}^{N} \dot{Q}^{\text{i,heat}}_k$, and the last term represents the heating loss depending on the temperature difference between storage and environment.

III. Distributed model predictive control for building demand-side management

In this section we present the proposed MPC framework. The proposed scheme is hierarchical. In the upper level, a trajectory planner calculates the best possible reachable power profile to track as reference. The afforded flexibility is optimised according to the time-varying economic incentives offered by the grid operator for increasing or decreasing the power demand with respect to a baseline. The reference can be updated at each time step. In the lower level, a tracking problem is solved. The cost function is divided into two terms, one penalizes the tracking error and the other one minimises the energy use without violating the indoor comfort.

A. Computation of the power reference

Here we present the upper level problem formulation. We assume that building energy users can participate in different balancing services as flexibility providers. They can be called to: *i)* either reduce their generation or increase their demand when there is an excess of energy in the system (denoted by BS^{UP}); *ii)* either increase their generation or decrease their demand when there is a deficit of energy (denoted as BS^{DOWN}). The following optimisation problem can be used to compute the afforded flexibility

$$\min \quad \sum_{k=0}^{T-1} \left(-c_k^{\text{UP}} \Delta P_k^{\text{UP}} + c_k^{\text{DOWN}} \Delta P_k^{\text{DOWN}} + c_k^{\text{gas}} \Delta P_k^{\text{gas}} \right)$$

s.t.

$$\begin{aligned}
&\Delta T_{k+1}^{\text{s}} = \Delta \dot{Q}_k^{\text{s}} - \textstyle\sum_{i=1}^{N} \Delta \dot{Q}_k^{i,\text{heat}} + \\
&\qquad -\text{h}_\text{s}\text{A}_\text{s}(T_k^{\text{s,BL}} + \Delta T_k^{\text{s}} - T_k^{\text{amb}}) \\
&\Delta \dot{Q}_k^{\text{s}} = \text{COP} \Delta P_k^{\text{HP}} + \eta^{\text{B}} \Delta P_k^{\text{gas,B}} + \eta^{\text{h}} \Delta P_k^{\text{gas,CHP}} \\
&\Delta P_k^{\text{gas}} = \Delta P_k^{\text{gas,CHP}} + \Delta P_k^{\text{gas,B}} \\
&\Delta P_k^{\text{grid}} = \Delta P_k^{\text{HP}} - \eta^{\text{e}} \Delta P_k^{\text{gas,CHP}} + \textstyle\sum_{i=1}^{N} \gamma^i \Delta \dot{Q}_k^{i,\text{heat}} \\
&T_k^{\text{DOWN}} \Delta P_k^{\text{DOWN}} \leq \Delta P_k^{\text{grid}} \leq T_k^{\text{UP}} \Delta P_k^{\text{UP}} \\
&\underline{\Delta \dot{Q}}_k^{i,\text{heat}} \leq \Delta \dot{Q}_k^{i,\text{heat}} \leq \overline{\Delta \dot{Q}}_k^{i,\text{heat}} \\
&-\overline{\Delta P}_k^{\text{DOWN}} \leq \Delta P_k^{\text{DOWN}} \leq -\underline{\Delta P}_k^{\text{DOWN}} \\
&\underline{\Delta P}_k^{\text{UP}} \leq \Delta P_k^{\text{UP}} \leq \overline{\Delta P}_k^{\text{UP}} \\
&\underline{\Delta P}_k^{\text{gas}} \leq \Delta P_k^{\text{gas}} \leq \overline{\Delta P}_k^{\text{gas}},
\end{aligned}$$

where $T_k^{\text{s,BL}}$ is the TES temperature at each time k resulting from baseline power and heat consumption, $\underline{\Delta \dot{Q}}_k^{i,\text{heat}}$ and $\overline{\Delta \dot{Q}}_k^{i,\text{heat}}$ are the acceptable flexibility in the heat requirements of each thermal zone i at each time k such that the indoor comfort is not violated. The binary numbers T_k^{DOWN}, T_k^{UP} model whether or not the availability window for BS^{DOWN} and BS^{UP} is active at time k, with $T_k^{\text{DOWN}} + T_k^{\text{UP}} \leq 1$ for each k (i.e., the grid operator does not ask the flexibility provider for both services at the same time). The optimal values of ΔP_k^{grid}, $\forall k$, represent the afforded flexibility, i.e. optimal deviations from the baseline power such that the profits are maximised and the thermal comfort is satisfied. The baseline power and heat consumptions and the bounds in Problem (1) can be estimated out of historical data [14].

B. Distributed MPC for reference tracking

We consider a star communication network, where we have a central node with more significant computing power, C-DG in Figure 1, and individual nodes, L-TZ in Figure 1, each corresponding to a thermal zone with local control inputs and limited computational resources [10]. The thermal zones have dynamics coupled only through the onsite generation and TES. However the thermal coupling between thermal zones is commonly negligible, a non negligible coupling can be handled by considering it as a disturbance term, as shown in [10].

Formulation of the MPC problem: We now present the formulation of the problem of tracking a reference power profile at minimum energy use without violating the thermal

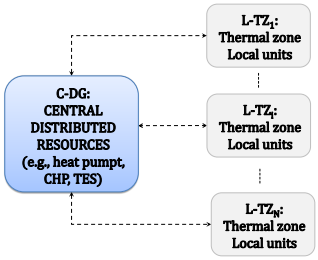

Fig. 1. Communication graph for the proposed distributed implementation.

comfort requirements. We first present the overall building model. The dynamics associated to each individual node L-TZ$_i$ can be written in compact form as

$$x_{k+1}^{\text{i}} = a^{\text{i}} x_k^{\text{i}} + b^{\text{i}} u_k^{\text{i}} + E^{\text{i}} w_k^{\text{i}} \tag{1}$$

where the scalars $a^{\text{i}}, b^{\text{i}}$ and the row vector E^{i} can be easily derived from Section II. In particular $x^{\text{i}} = T^{\text{i,a}}$, $u^{\text{i}} = \dot{Q}^{\text{i,heat}}$ and $w^{\text{i}} = [T^{\text{ext}}, I^{\text{i}}, N^{\text{i,people}}]'$.

The dynamics associated to the central node C-DG can be written in compact form as

$$x_{k+1}^{\text{s}} = a^{\text{s}} x_k^{\text{s}} + B^{\text{s}} u_k^{\text{s}} - \mathbf{1}_N \boldsymbol{u}_k^{\text{zone}} + e^{\text{s}} w_k^{\text{s}}, \tag{2}$$

where the scalars $a^{\text{s}}, e^{\text{s}}$ and the row vector B^{s} can be easily derived from Section II, $\mathbf{1}_N$ is a row vector with N 1's elements and $\boldsymbol{u}^{\text{zone}}$ is the column vector of the stacked inputs to the thermal zones. In particular $x^{\text{s}} = T^{\text{s}}$, $u^{\text{s}} = [P^{\text{HP}} \quad P^{\text{gas,B}} \quad P^{\text{gas,CHP}}]'$, $w^{\text{s}} = T^{\text{amb}}$ and $B^{\text{s}} = [\text{COP} \quad \eta^{\text{B}} \quad \eta^{\text{h}}]$.

At each time step k we define $\boldsymbol{x}_k := \left[x_k^1, \dots, x_k^N \quad x_k^{\text{s}}\right]'$, $\boldsymbol{u}_k := \left[\boldsymbol{u}_k^{\text{zone}'} \quad u_k^{\text{s}}\right]'$ and $\boldsymbol{w}_k := \left[w_k^{1'}, \dots, w_k^{N'} \quad w_k^{\text{s}}\right]'$.

Then the overall building model can be written in a compact form as

$$\boldsymbol{x}_{k+1} = \boldsymbol{A}\boldsymbol{x}_k + \boldsymbol{B}\boldsymbol{u}_k + \boldsymbol{E}\boldsymbol{w}_k, \tag{3}$$

where $\boldsymbol{A} = \text{diag}\,(a^1, \dots, a^N, a^{\text{s}})$, $\boldsymbol{E} = \text{diag}\,(E^1, \dots, E^N, e^{\text{s}})$ and

$$\boldsymbol{B} := \begin{bmatrix} b^1 & 0 & \dots & \mathbf{0}_{1\times 3} \\ 0 & \ddots & & \vdots \\ \vdots & & b^N & \\ -1 & \dots & -1 & B^{\text{s}} \end{bmatrix}$$

Equality and inequality constraints: We now denote the state and input trajectories over the prediction horizon T respectively by $\boldsymbol{x} := \left[\boldsymbol{x}_1', \dots, \boldsymbol{x}_T'\right]'$ and $\boldsymbol{u} := \left[\boldsymbol{u}_0', \dots, \boldsymbol{u}_{T-1}'\right]'$. We then define $\boldsymbol{z} := \left[\boldsymbol{x}', \boldsymbol{u}'\right]'$. The propagation of the system dynamics (3) over the prediction horizon T generates the following equality constraints

$$\boldsymbol{F}\boldsymbol{z} = \boldsymbol{f}, \tag{4}$$

where

$$\boldsymbol{F} := \begin{bmatrix} \boldsymbol{I} & \boldsymbol{0} & \dots & \boldsymbol{0} & -\boldsymbol{B} & \boldsymbol{0} & \dots & \boldsymbol{0} \\ -\boldsymbol{A} & \boldsymbol{I} & \dots & \boldsymbol{0} & \dots & -\boldsymbol{B} & \dots & \boldsymbol{0} \\ \boldsymbol{0} & \dots & \ddots & \vdots & \vdots & & \ddots & \vdots \\ \boldsymbol{0} & \dots & -\boldsymbol{A} & \boldsymbol{I} & \boldsymbol{0} & \dots & & -\boldsymbol{B} \end{bmatrix}$$

$$\boldsymbol{f} := \begin{bmatrix} \boldsymbol{A}\boldsymbol{x}_0 + \boldsymbol{E}\boldsymbol{w}_0 \\ \boldsymbol{E}\boldsymbol{w}_1 \\ \vdots \\ \boldsymbol{E}\boldsymbol{w}_{T-1}. \end{bmatrix}$$

We point out that $\boldsymbol{F} \in \mathcal{R}^{T(N+1)\times T(2N+4)}$ is a wide matrix and has full rank, as required in [9], since $\boldsymbol{B}$ has full row rank. We also include polytopic constraints on states and inputs, $\underline{\boldsymbol{z}} \leq \boldsymbol{z} \leq \overline{\boldsymbol{z}}$, where $\underline{\boldsymbol{z}}$ and $\overline{\boldsymbol{z}}$ contain comfort ranges for the indoor temperatures and bounds on TES temperature and on the control inputs, as defined in Table I. We now assume that a reserve call occurs at the current point in time, $k = 0$. In order to account for the reference power signal to track we include an additional inequality constraint for each time k, $P_k^{r,\text{grid}} - \epsilon_k^{\text{grid}} \leq P_k^{\text{grid}} \leq P_k^{r,\text{grid}} + \epsilon_k^{\text{grid}}$, where $P_k^{\text{grid}} = P_k^{\text{HP}} - \eta^{\text{e}} P_k^{\text{gas,CHP}} = F^{\text{grid}} \boldsymbol{u}_k$, with $F^{\text{grid}} = [0, \dots, 0 \quad 1 \quad 0 \quad -\eta_{\text{e}}]$, is the electrical power exchanged with the grid and $\epsilon_k^{\text{grid}} \geq 0$ represents the deviation from the reference signal at time k. Each variable ϵ_k^{grid} is highly penalised in the objective function. Notice that additional distributed generators, such as photovoltaic plants, can be easily included by modifying the power balance as follows: $P_k^{\text{grid}} = P^{\text{HP}} - \eta_{\text{e}} P^{\text{gas,CHP}} - P^{\text{PV}}$, where P^{PV} is handled as disturbance and replaced by forecasts. The power signal to track, $\boldsymbol{P}^{r,\text{grid}}$, is computed by solving the problem (1). The reference power signal is to be followed over a previously agreed temporal window T at each $k = 0, \dots, T-1$ with the grid operator. The service provider (the building in this case) committed to be available during a T and offer a certain amount of flexibility.

Remark 3: It is possible to include in P_k^{grid} additional electrical power consumption associated with each $\dot{Q}_k^{\text{i,heat}}$ (e.g., power required by fan, pumps and compressors of HVAC systems), which can be estimated by using data-driven approach based on logged measurement data.

Constraints (**??**) over T can be written in a compact form as

$$\begin{aligned} \boldsymbol{F}^{\text{grid}} \boldsymbol{z} - \boldsymbol{\epsilon}^{\text{grid}} &\leq \boldsymbol{P}^{r,\text{grid}} \\ -\boldsymbol{F}^{\text{grid}} \boldsymbol{z} + \boldsymbol{\epsilon}^{\text{grid}} &\leq -\boldsymbol{P}^{r,\text{grid}}, \end{aligned} \tag{5}$$

where $\boldsymbol{F}^{\text{grid}} = [\boldsymbol{0} | \text{ diag } (F^{\text{grid}}, \dots, F^{\text{grid}})]$, with $\boldsymbol{0}$ a matrix of zero's of appropriate size.

We augment the vector $\boldsymbol{z}$ by including the column vector $\boldsymbol{\epsilon}^{\text{grid}}$ of stacked ϵ_k^{grid} over T and define $\boldsymbol{z}_{\text{grid}} := \left[\boldsymbol{z}^{'}, \boldsymbol{\epsilon}^{\text{grid}^{'}}\right]^{'}$. Hence, constraints (5) can be further re-written as $\boldsymbol{K}^{\text{grid}} \boldsymbol{z}_{\text{grid}} \leq \boldsymbol{k}^{\text{grid}}$, where $\boldsymbol{K}^{\text{grid}}$ is a matrix of appropriate size and $\boldsymbol{k}^{\text{grid}}$ is a column vector containing stacked positive and negative values of the reference power signal $\boldsymbol{P}^{r,\text{grid}}$.

Objective function: The quadratic cost function we consider in order to minimise the energy use is

$$J = \frac{1}{2} \boldsymbol{x}^{'} \boldsymbol{S} \boldsymbol{x} + \boldsymbol{u}^{'} \boldsymbol{R} \boldsymbol{u}, \tag{6}$$

where the diagonal and definite positive matrices $\boldsymbol{S}$ and $\boldsymbol{R}$ represents penalties on states and on inputs. We point out that the penalty on states will be lower than the penalty on the inputs. The Hessian matrix $\boldsymbol{H}$ is given by $\boldsymbol{H} =$ diag $(\boldsymbol{S}, \boldsymbol{R})$. Then the objective function can be re-written as $J = \frac{1}{2} \boldsymbol{z}^{'} \boldsymbol{H} \boldsymbol{z}$. We can then modify matrix $\boldsymbol{H}$ such to include the penalty on the deviations from the reference signal, $\boldsymbol{R}^{\text{grid}}$, as follows $\boldsymbol{H}_{\text{grid}} =$ diag $(\boldsymbol{S}, \boldsymbol{R}, \boldsymbol{R}^{\text{grid}})$. In order to apply the active-set algorithm illustrated in [9], we have to convert the additional inequality constraints (5) into equality constraints by introducing positive slack variables $\boldsymbol{\sigma}$: $\boldsymbol{K}^{\text{grid}} \boldsymbol{z}_{\text{grid}} + \boldsymbol{\sigma} = \boldsymbol{k}^{\text{grid}}$. The vector of decision variables has to include also the slack variables but this implies that $\boldsymbol{H}_{\text{grid}}$ is positive semi-definite and not positive definite. In order to address this issues, as proposed in [10], we add a Lagrangian penalty to the cost function J for the introduced equality constraints. The Hessian of J is accordingly modified as follows

$$\boldsymbol{H}_{\text{aug}} := \begin{bmatrix} \boldsymbol{H}_{\text{grid}} + \rho \boldsymbol{K}^{\text{grid}^{'}} \boldsymbol{K}^{\text{grid}} & \boldsymbol{K}^{\text{grid}^{'}} \\ \boldsymbol{K}^{\text{grid}} & \boldsymbol{I} \end{bmatrix},$$

which is positive definite. The penalty factor ρ is greater or equal to 1.

Finally, the MPC problem can be formulated as the following strictly convex quadratic problem

$$\begin{aligned} \min_{\boldsymbol{z}_{\text{aug}}} \quad & \tfrac{1}{2} \boldsymbol{z}_{\text{aug}}^{'} \boldsymbol{H}_{\text{aug}} \boldsymbol{z}_{\text{aug}} \\ \text{s.t.} \quad & \\ & \boldsymbol{F}_{\text{aug}} \boldsymbol{z}_{\text{aug}} = \boldsymbol{f}_{\text{aug}} \\ & \underline{\boldsymbol{z}}_{\text{aug}} \leq \boldsymbol{z}_{\text{aug}} \leq \overline{\boldsymbol{z}}_{\text{aug}}, \end{aligned} \tag{7}$$

where $\boldsymbol{z}_{\text{aug}}$ is the vector $\boldsymbol{z}_{\text{grid}}$ stacked with the slack variables $\boldsymbol{\sigma}$, $\boldsymbol{F}_{\text{aug}}$ and $\boldsymbol{f}_{\text{aug}}$ are respectively the matrix $\boldsymbol{F}$ and the column vector $\boldsymbol{f}$ from (4) appropriately modified to include the introduced decision variables $\boldsymbol{\epsilon}^{\text{grid}}$ and $\boldsymbol{\sigma}$. The polytopic constraints representing bounds on all the decision variables are also accordingly augmented. Problem (7) can be solved by using the active-set method proposed in [9]. In the case study presented in Section IV the convergence is generally achieved after two or three iterations. We point out that it is possible to tune the tradeoff between the energy use and the reference tracking by appropriately tuning the penalty on the inputs and on the variables representing the deviation from the reference power signal. Further, the MPC problem can be easily extended to soften the thermal comfort constraints and increase the available flexibility.

Distributed implementation: Similarly to [10], we can solve the problem (7) by applying the active-set algorithm in [9] in a distributed fashion. At each iteration, the active-set method generates a sequence of subsets of inequality constraints which are active (i.e. they are satisfied with equality at the optimum) and finds the inactive primal variables and the dual variables corresponding to the equality

constraints by solving a subspace minimisation. In the distributed implementation, the dual variables and the active sets corresponding to TES and onsite generation are updated in the central node C-DG (see Figure 1), while each node L-TZ$_i$ finds its corresponding dual variables and active sets; these calculations occur in parallel and do not require powerful computing units. The subspace minimisation is solved in the central node. We propose a simple initialisation algorithm for our MPC problem, summarised in Algorithm 1. In the first step of Algorithm 1, $\boldsymbol{u}_k$, $\forall k$, are computed as follows

$$\begin{aligned} &\text{if} \quad P_k^{r,\text{grid}} < 0, \quad P_k^{\text{gas},CHP} = \frac{P_k^{r,\text{grid}}}{\eta_{\text{e}}} \\ &\qquad\qquad u_k^{\text{s}} = \eta_{\text{h}} P_k^{\text{gas},CHP}, \quad u_k^{\text{i}} = \frac{u_k^{\text{s}}}{N} \\ &\text{if} \quad P_k^{r,\text{grid}} \geq 0, \quad P_k^{\text{HP}} = P_k^{r,\text{grid}} \\ &\qquad\qquad u_k^{\text{s}} = \eta \text{COP} P_k^{\text{HP}}, \quad u_k^{\text{i}} = \frac{u_k^{\text{s}}}{N} \end{aligned} \tag{8}$$

Algorithm 1 Initialisation Algorithm

1: Set $\boldsymbol{u}_k$, $\forall k$, using (8) and $\epsilon_k^{\text{grid}} = 0$
2: Each node L-TZ$_i$ obtains the states, x_k^i, $\forall k$, using (1)
3: C-DG obtains the states, $\boldsymbol{x}_k^{\text{s}}$, $\forall k$, using (2)
4: $\overline{\mathcal{A}}_0 = \cup_i \{j : x_j^i > \overline{x}_j^i\} \cup \{j : x_j^{\text{s}} > \overline{x}_j^{\text{s}}\}$
5: $\underline{\mathcal{A}}_0 = \cup_i \{j : x_j^i < \underline{x}_j^i\} \cup \{j : x_j^{\text{s}} < \underline{x}_j^{\text{s}}\}$
6: $\mathcal{I}_0 = \{j : j \notin \overline{\mathcal{A}}_0 \cup \underline{\mathcal{A}}_0\}$.

Proposition 1: Consider Problem (7) and assume it is feasible. Then Algorithm 1 satisfies the feasibility condition $\mathcal{Z}_{\mathcal{I}} \neq \emptyset$

Proof: Matrix F$_{\text{aug}}$ is still a wide matrix, since we augmented F with $2T$ variables and included $2T$ equality constraints. This matrix will be given by $\begin{bmatrix} \text{F} & \boldsymbol{0} \\ \text{K}^{\text{grid}} & \boldsymbol{I} \end{bmatrix}$. Algorithm 1 will remove some columns from the first $T(N+1)$ columns of F$_{\text{aug}}$, which corresponds to the active elements of $\boldsymbol{x}$. The matrix F$_{\text{aug},\mathcal{I}}$ will still include the block diagonal matrix $\boldsymbol{B}$ and the identity matrix $\boldsymbol{I}$, hence it will be full row rank. Therefore, $\mathcal{Z}_{\mathcal{I}} \neq \emptyset$ ■

IV. Numerical Evaluation

In this section we present the numerical evaluation of the methodology presented in Section III. The proposed approach is applied to a 4-storey university building in the University of Manchester campus, consisting of several rooms and laboratories. The building is equipped with three air handling units (AHU) located on the top floor and supplying ventilation to different areas of the building according to their use, i.e. common areas, laboratories and pilot plants. Variable-air-volume (VAV) terminals supply the air to the thermal zone under control. For each one of the AHUs, the supplied air is heated through hot water coils with hot water provided by a thermal energy storage (TES). The TES is fed through a ground source heat pump (GSHP) and backed up by a set of two boilers.

A. Simulation Setup

In order to test the developed control strategy, the building, with its components and energy equipment, is accurately modelled by using the building energy simulation software EnergyPlus (E+). The interface between E+ and MATLAB is implemented by using the MLE+ library. As mentioned above, the heat is provided by two boilers and the TES, connected to the GSHP and the boilers loops. The temperature of the hot water inside the TES has to be kept within a given range. The GSHP and the TES serves the entire building and are assigned to the central node C-DG (see Figure 1). The TES water temperature is modelled as in (2), where the input vector is $u^{\text{s}} = \begin{bmatrix} P^{\text{HP}} & P^{\text{gas,B}} \end{bmatrix}'$. The elements of the input vector can be seen as the heat pump (HP) power and the aggregated boilers (B) power consumed. Each of the thermal zones served by each of the three AHUs is modelled as in (1) and is assigned to the local node L-TZ$_i$ (see Figure 1). The heat to be provided by each AHU to meet the comfort requirements of the corresponding thermal zone, $u^{\text{i}} = \dot{Q}^{\text{i,heat}}$, is fed from the heat pump, $\dot{Q}_k^{\text{HP}} = \text{COP} P_k^{\text{HP}}$, and the boilers, $\dot{Q}_k^{\text{B}} = \eta^{\text{B}} P_k^{\text{gas,B}}$, through the thermal storage. The dynamics of the TES and thermal zones are identified by applying a pseudorandom binary signal (PRBS) to the corresponding actuators affecting their dynamics. Outside temperature, occupancy and solar radiation data of the actual building location is utilised for performing the identification task. Figure 2 shows the model validation results of the TES and one thermal zone (the other two zones exhibit similar profiles). We can see that the identified model responses capture well enough the main dynamics of the actual TES and thermal zone.

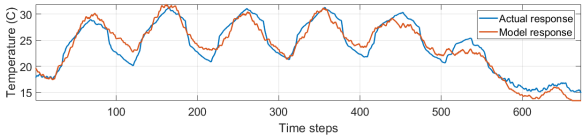

(a)

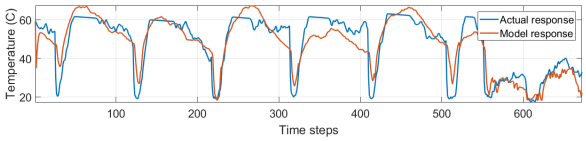

(b)

Fig. 2. Comparison of the actual and identified model responses for the thermal dynamics of one thermal zone (a) and the TES (b).

B. Result Evaluation

The MPC for demand side management algorithm, denoted by MPC-DSM, is implemented in MATLAB and the first week of April 2017 is considered for conducting the numerical experiment. The longest computational time of MPC iterations is 0.687 seconds on a Windows system Core i7 @ 2.80 GHz. The reference power profile in Fig. 4 is obtained by solving Problem (1). Forecasts of the disturbances are based on E+ building simulations and weather forecasts. The heat inputs to each thermal zone and the power setpoints to the GSHP and the TES are computed as described in Section III and then applied to the E+ building model at each MPC iteration. The zone temperature comfort range is set between 19°C and 23°C between 8:00 am and 5:45 pm.

The bounds on the TES water temperature are set to 60°C and 70°C during the same time interval. The sampling time is 15 minutes and the prediction horizon of the MPC problem is 48 steps (12 hours ahead). Fig. 3 shows the different temperature profiles resulting by the E+ baseline rule-based control system, $\text{RBC}_{\text{E+}}$, and our MPC-based control system, MPC-DSM. The thermal bounds and the actual disturbance profiles of the first week of April 2017 are also depicted.

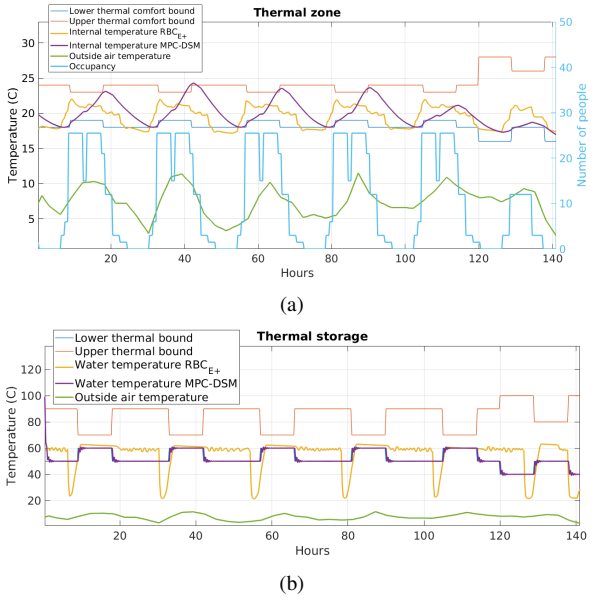

Fig. 3. Comparison between the baseline rule-based control and the MPC-DSM for one thermal zone (a) and for the TES (b).

Fig. 4 depicts the reference power signal and the power profile resulting from the MPC-DSM. The power reference profile exhibits a decrease in the power exchanged with the grid during peak hours, in early afternoon, and over the weekend. Fig. 4 shows that the reference is reasonably followed by the building power profile without violating both the thermal zone comfort bounds and the limits on the TES water temperature, as illustrated by Fig. 3, whilst the temperature profiles resulting from the $\text{RBC}_{\text{E+}}$ violate the bounds, significantly in case of the TES. We recall that

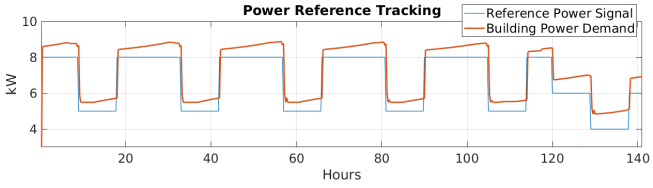

Fig. 4. Reference and building power profiles.

the comfort bounds are not softened and the tracking results depend on the penalty on the decision variables representing the deviation from the reference signal, ϵ^{grid}. In this case, the comfort has priority and the building is not able to exactly follow the computed reference power profile.

V. Conclusions and Future Studies

In this paper, we propose a hierarchical Model Predictive Control (MPC) framework for building demand-side management while minimising the energy use without violating the indoor thermal comfort.

Building on the work in [9], [10], we propose a distributed implementation of the MPC problem. Furthermore, we present a suitable initialisation algorithm. Practical implementation can benefit from the distributed approach of the proposed control framework. Numerical results based on real measurements from an actual university building show promising results. Future works will include the extension of the modeling to include more complex building dynamics and additional onsite generation, as well as the extension of the control framework to incorporate statistics of the disturbances, based on historical data. Another relevant direction is to investigate suitable tuning strategies of penalty on the inputs, in particular the tradeoff between the energy use and the tracking of the reference power signal.

References

[1] T. Samad, E. Koch, and P. Stluka, "Automated demand response for smart buildings and microgrids: The state of the practice and research challenges," *Proceedings of the IEEE*, vol. 104, no. 4, pp. 726–744, April 2016.

[2] F. Lamnabhi-Lagarrigue, A. Annaswamy, S. Engell, A. Isaksson, P. Khargonekar, R. M. Murray, H. Nijmeijer, T. Samad, D. Tilbury, and P. V. den Hof, "Systems & control for the future of humanity, research agenda: Current and future roles, impact and grand challenges," *Annual Reviews in Control*, vol. 43, no. Supplement C, pp. 1 – 64, 2017.

[3] M. Morari, J. Lee, and C. Garcia, *Model Predictive Control*. Prentice Hall, 2001.

[4] H. Thieblemont, F. Haghighat, R. Ooka, and A. Moreau, "Predictive control strategies based on weather forecast in buildings with energy storage system: A review of the state-of-the art," *Energy and Buildings*, vol. 153, no. Supplement C, pp. 485 – 500, 2017.

[5] S. S. Walker, W. Lombardi, S. Lesecq, and S. Roshany-Yamchi, "Application of distributed model predictive approaches to temperature and co2 concentration control in buildings," *IFAC-PapersOnLine*, vol. 50, no. 1, pp. 2589 – 2594, 2017.

[6] X. Hou, Y. Xiao, J. Cai, J. Hu, and J. E. Braun, "Distributed model predictive control via proximal jacobian admm for building control applications," in *2017 American Control Conference (ACC)*, May 2017, pp. 37–43.

[7] L. Fabietti, T. Gorecki, F. Qureshi, A. Bitlislioglu, I. Lymperopoulos, and C. Jones, "Experimental implementation of frequency regulation services using commercial buildings," *IEEE Transactions on Smart Grid*, vol. PP, no. 99, pp. 1–1, 2017.

[8] M. Kramer, A. Jambagi, and V. Cheng, "A model predictive control approach for demand side management of residential power to heat technologies," in *2016 IEEE International Energy Conference (ENERGYCON)*, April 2016, pp. 1–6.

[9] F. Curtis, Z. Han, and D. Robinson, "A globally convergent primal-dual active-set framework for large-scale convex quadratic optimization," *Computational Optimization and Applications*, vol. 60, no. 2, pp. 311–341, March 2015.

[10] S. Koehler, C. Danielson, and F. Borrelli, "A primal-dual active-set method for distributed model predictive control," *Optimal Control Applications and Methods*, vol. 38, no. 3, pp. 399–419, June 2016.

[11] A. Parisio, C. Wiezorek, T. Kyntäjä, J. Elo, K. Strunz, and K. H. Johansson, "Cooperative MPC-Based Energy Management for Networked Microgrids," *IEEE Transactions on Smart Grid*, vol. 8, no. 6, pp. 3066–3074, Nov 2017.

[12] A. Bloess, W. Schill, and A. Zerrahn, "Power-to-Heat for Renewable Energy Integration: Technologies, Modeling Approaches, and Flexibility Potentials," German Institute for Economic Research, Tech. Rep., 2017.

[13] B. Thomas, "Benchmark testing of micro-chp units," *Applied Thermal Engineering*, vol. 28, no. 16, pp. 2049 – 2054, 2008.

[14] S. Bhattacharya, "Baseline Building Power Estimation," Electrical Engineering and Computer Sciences University of California at Berkeley, Tech. Rep. UCB/EECS-2017-45, May 2017.